Contents

Chapter 4

Electron beam

The performance of the photon source is dependent upon the parameters of the electron beam in several important areas. These parameters are listed in Table 4.1. The first column of numbers gives the set of parameters that have been adopted as the design goals for the source. These are the values that have been taken as input in calculating the characteristics of the coherent bremsstrahlung source. The second column of numbers was obtained from a concrete design of the HALL D beam line [1] that was carried out by members of the Jefferson Lab Accelerator Division. The exact choice of the final parameters has not yet been made, but the preliminary design shows that all of the design goals can be met within the available real estate. The reduction of the radiator-collimator distance from $80\,m$ to $75\,m$ does not significantly affect the performance of the source.

The following sections highlight the particular properties of the electron beam which have a special impact on the performance of the source.

4.1 Beam polarization

It has already been stated that to generate bremsstrahlung photons with linear polarization it is necessary to use an oriented crystal radiator. However photons with circular polarization are produced by ordinary incoherent bremsstrahlung any time the incident electrons are longitudinally polarized. In fact for $9 GeV$ photons produced by $12 GeV$ electrons, the transfer from electron beam longitudinal polarization to photon beam circular polarization is greater than 80%. This raises the question of what happens when one has longitudinally-polarized electrons incident on an oriented crystal radiator. What happens in this case is that the photon beam is elliptically polarized; it

parameter	design goals	design results
energy	12 GeV	12 GeV
electron polarization	not required	available
minimum useful current	100 pA	100 pA
maximum useful current	3 μA	5 μA
r.m.s. energy spread	< 10 MeV	7 MeV
transverse x emittance	10 $mm \cdot \mu$r	10 $mm \cdot \mu$r
transverse y emittance	2.5 $mm \cdot \mu$r	2.3 $mm \cdot \mu$r
x-dispersion at radiator	none	negligible
y-dispersion at radiator	none	$<$ 1cm
x spot size at radiator	1.7 mm r.m.s.	1.55 mm r.m.s.
y spot size at radiator	0.7 mm r.m.s.	0.55 mm r.m.s.
x image size at collimator	0.5 mm r.m.s.	0.54 mm r.m.s.
y image size at collimator	0.5 mm r.m.s.	0.52 mm r.m.s.
distance radiator to collimator	80 m	75 m
position stability	± 200 μm	

Table 4.1: Electron beam properties that were asked for (column 2) and obtained (column 3) in a preliminary optics design for the transport line connecting the accelerator to the Hall D photon source.

carries both circular and linear polarization. There is a sum rule that limits the sum of the squares of the linear plus circular polarizations to be no greater than 1. Hence one sees the linear polarization in coherent bremsstrahlung going to zero as one approaches the end-point energy (see Fig. **??**) while at the same time the circular polarization goes to 1 at the end-point (assuming electrons of 100% longitudinal polarization).

The statement in Table 4.1 that electron beam polarization is not required for the GlueX experiment in Hall D is correct, but it is not correct to assume that the photon source is independent of the state of polarization of the electron beam. The presence of a non-zero circular polarization in the Hall D photon beam will, in principle, produce observable effects in the angular distributions measured in photoproduction reactions. This means that there will be an important coupling between the GlueX program and the other experimental halls whose programs sometimes require them to have control over the beam polarization. This coupling can be eliminated by setting up the tune of the electron beam line to Hall D such that the longitudinal component of the electron beam polarization is rotated to zero at the crystal radiator. Whether the decision is made to rotate it away or simply to measure its value periodically, this consideration underlines the importance of having a means to measure photon beam polarization in a way that does not rely on *a priori* knowledge of the properties of the electron beam.

Although the ability of the source to produce photon beams with both circular and linear polarization complicates operation when one of them is desired without the other, it does increase the versatility of the source. The two kinds of polarization are controlled independently of one other, and together they give access to a more complete set of polarization observables than would be possible with only one or the other.

4.2 Beam emittance

The values for the electron beam emittances shown in Table 4.1 are estimates based upon the parameters of the current machine projected to $12GeV$[1]. The definition of emittance used here is the product of the r.m.s. widths of the beam in transverse position and divergence angle. Because synchrotron radiation inside the accelerator occurs mainly in the horizontal plane, the emittance values in x are generally larger than those for y. The two vertical bends required for bringing the $12GeV$ beam from the level of the accelerator up to beam height in Hall D do increase the vertical emittance a small amount over its value inside the machine; this effect has been included in computing the vertical emittance shown in Table 4.1.

The longitudinal emittance of the beam is important as it is the limiting factor in determining the ultimate energy resolution of the tagger. The design goal of 0.1% photon energy resolution is well matched to the energy spread expected for the CEBAF beam at $12 GeV$.

The place where transverse emittance plays a critical role is at the photon collimator. For optimum effectiveness in collimation it is important that the virtual electron beam spot at the collimator position be as small as possible. The electron beam does not actually reach the photon collimator, being bent into the dump by the tagger magnet shortly after the radiator. But considering the optics of the electron beam as if the tagger dipole were switched off, the electron beam at the radiator can be projected forward to form a virtual image on the collimator entrance plane. The position and size of this virtual spot determines the definition of 0° emission angle for the photons. If this spot is small compared to the collimator aperture and is correctly centered then the bremsstrahlung photons of a given emission angle α intersect the entrance plane of the collimator in a well-defined ring of radius $D\alpha$ concentric with the collimator aperture, where D is the distance between the radiator and the collimator entrance plane. In this way a collimator of diameter d passes only those photons of emission angle $\alpha \leq d/2D$. If however the size of the virtual spot is comparable to or larger than the collimator aperture then the ring image of photons of a given emission angle α is smeared out, so that the effect of collimation is simply to reduce the intensity of the beam but not to enhance the coherent component.

Note that this analysis does not place any specific limits on the size of the beam at the radiator. The beam spot can and should be larger there to increase the lifetime of the crystal between spot moves. For the SLAC coherent bremsstrahlung source the beam spot at the radiator was about $2\,mm$ r.m.s. focused down to a $1\,mm$ r.m.s. virtual spot at the primary collimator positioned $91\,m$ downstream of the radiator.

The superior emittance characteristics of the CEBAF beam allow the transverse dimensions to be somewhat smaller than this for the HALL D source, more so in the vertical than the horizontal dimension. The difference between the horizontal and vertical emittance of the CEBAF beam implies that making the spot round at the radiator implies an elliptical virtual spot at the collimator, and *vice versa*. It is difficult to construct a collimator with an elliptical aperture, so the choice was made to make the virtual spot round. This is why the beam spot on the radiator is asymmetric.

Figure 4.1 shows how the collimated photon spectrum depends upon the transverse emittance of the electron beam. To generate this plot the increases

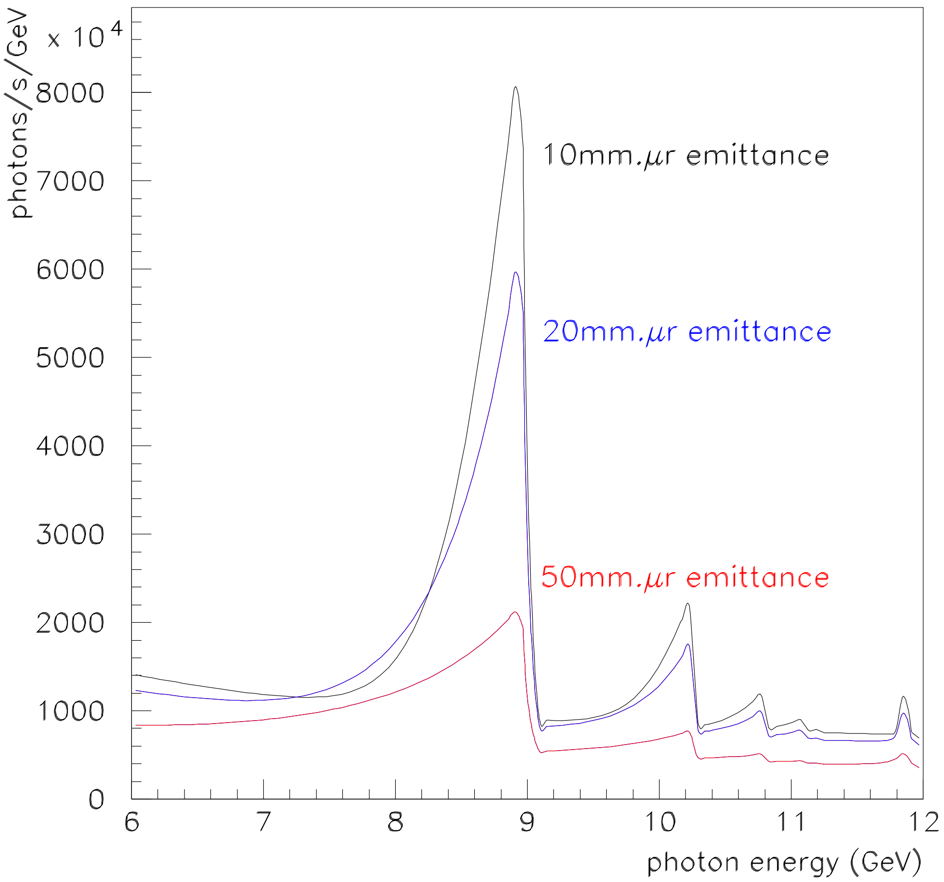

Figure 4.1: Coherent photon spectrum for three different values of the electron beam transverse emittance. The horizontal (shown on the plot) and vertical emittances are assumed to scale together. A 3.4 mm collimator located 80 m from the radiator was used for this calculation.

in emittance were simply translated into an increased virtual spot size on the collimator. This was done because it was assumed that the spot size of the electron beam on the radiator, already close to $2\,mm$ r.m.s., cannot be further inflated and stay contained within the limits of the crystal. When the virtual spot size becomes comparable with the collimator aperture then the collimation is rendered ineffective, and the photon spectrum and polarization revert to their uncollimated values. There is another connection between focal spot size and beam emittance that is connected with the requirement that all electrons enter the radiator at the same incidence angle with respect to the planes of the crystal. Practically, the divergence does not broaden the coherent peak provided that it is kept below the mosaic spread of the crystal. A conservative value for the allowable angular divergence δ in the electron beam at the radiator would then be 20 μr . Taken together with a $500\,\mu m$ r.m.s. spot size at the focus, this leads to an emittance of $10\,mm{\cdot}\mu r$ at $12 GeV$. This corresponds to the upper curve in Fig. 4.1.

4.3 Electron beam line optics

Translating the beam emittance into r.m.s. values for the beam radius and divergence requires the knowledge of the β function of the transport line between the accelerator and the radiator, defined as the ratio of the beam size to its angular divergence.

The preliminary optics design [1] of the Hall D beam line (see Table 4.1) is shown in Fig. 4.2. The horizontal and vertical beta functions are shown in the upper and lower panels, respectively. Between the two panels is shown a schematic of the transport lattice. The design begins at the exit of the beam from the end of the linac and ends at Hall D. The z coordinate is measured along the axis of the linac, with its origin at the mid-point of the accelerator. Fig. 4.3 shows the beta functions translated into r.m.s. beam size and shifted to place the radiator at the origin. The design allows the ratio of the spot sizes at the radiator and collimator to be adjusted over about an order of magnitude simply by changing the current in the beam line elements. In this way it will be possible to optimize the optics for a given size of crystal and collimator after beams are delivered to the hall, and more precise values for the emittances are in hand.

Not only must the virtual electron spot be small enough to fit within the collimator aperture, but it must also be centered on the aperture and stable. In order to maintain a stable beam position on the collimator, the SLAC experiment [2] instrumented the collimator with a secondary-emission detec-

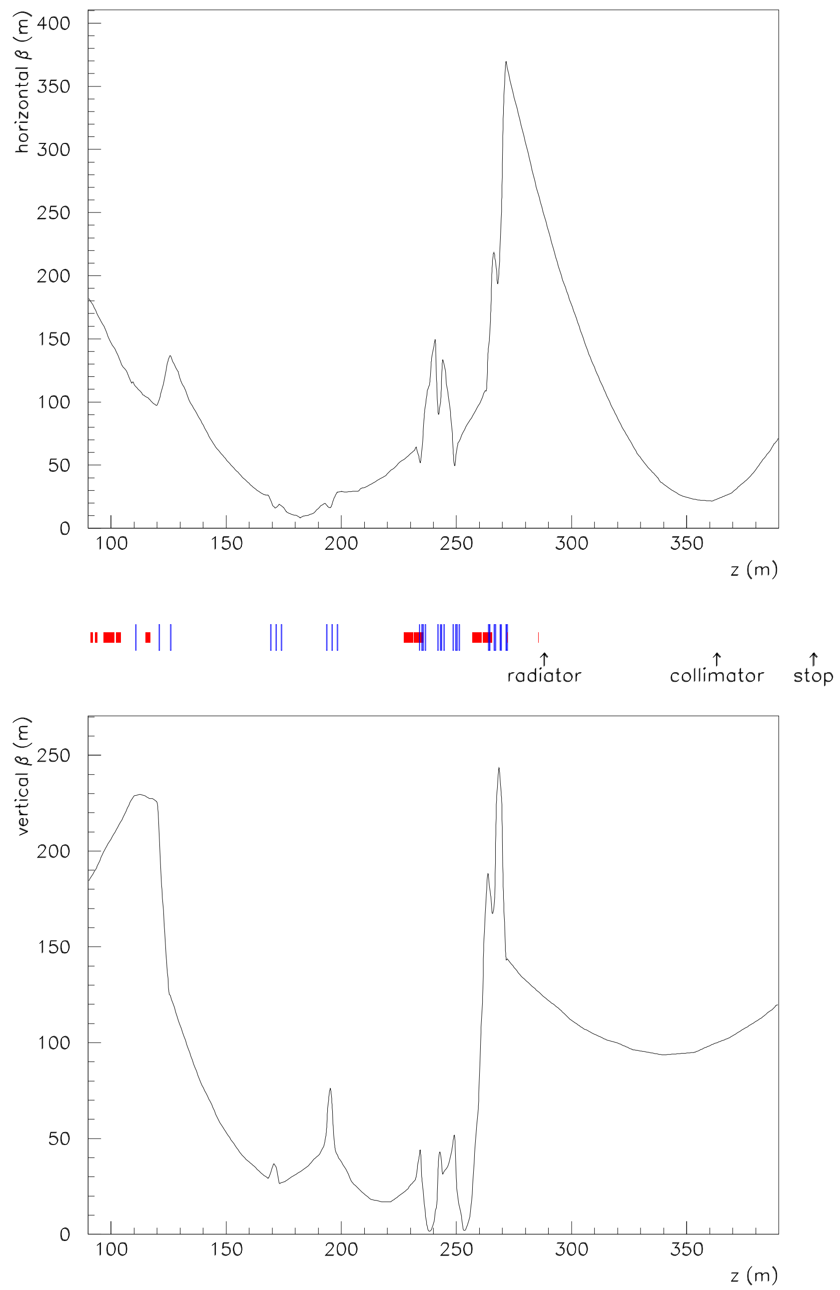

Figure 4.2: Horizontal (upper panel) and vertical (lower panel) beta functions from the preliminary optics design for the transport line from the accelerator to the Hall D photon source. The beam line lattice is shown schematically between the two panels, with dipole magnets represented by the short boxes and quadrupoles by the taller lines. The z coordinate is equal to the flight path length of the electrons starting at the center of the linac, up to an error of a few cm from the vertical motion of the beam.

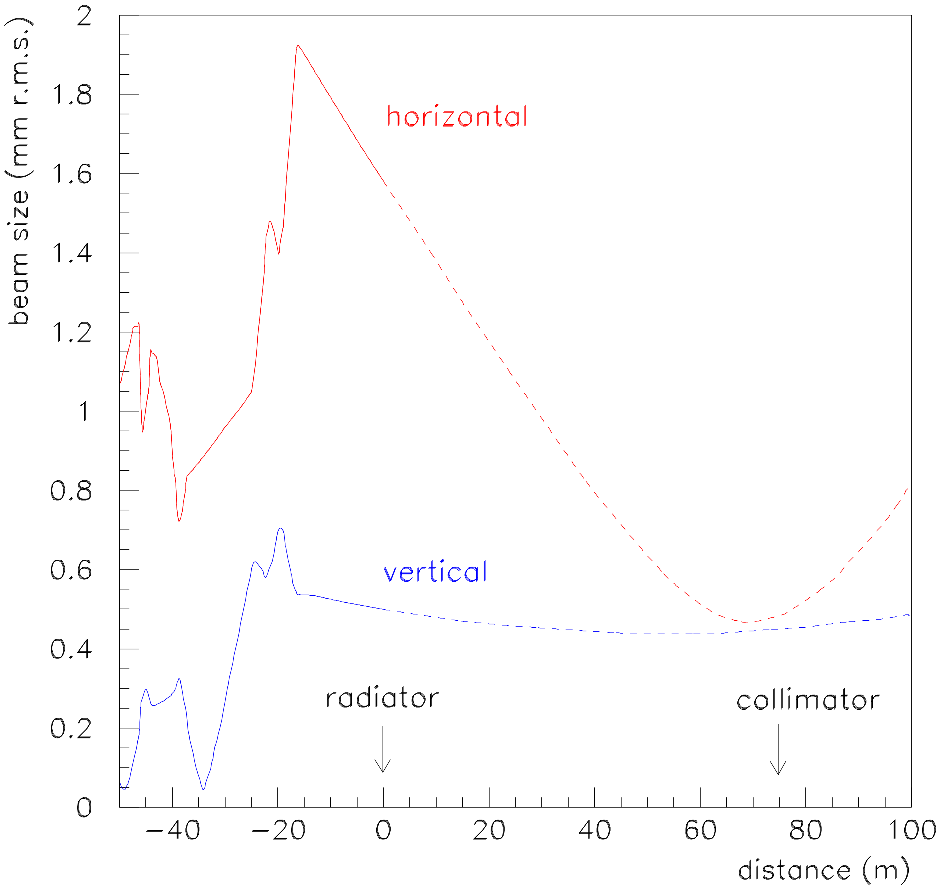

Figure 4.3: Horizontal and vertical r.m.s. envelopes for the electron beam in the region of the photon source, as derived from the beam emittance and beta functions of Fig. 4.2. The origin of the z coordinate has been placed at the radiator. In the region between the radiator and the collimator the envelope refers to the projected image of the electron beam, and does not describe the size of a physical beam that exists in that region.

tor. The detector was of the "pin-cushion" design and was installed between segments of the collimator near the position of the shower maximum. The readout was divided into four quadrants, which read equal currents when the beam was properly aligned on the collimator. The readout was connected via a feedback loop to the last steering elements on the electron beam line prior to the radiator. Over that distance a bend of only 10 μr results in a shift of $1\,mm$ at the collimator position. The small deflections that are necessary to keep the beam centered on the collimator do not produce appreciable walk in the beam-crystal angle. This means that an active feedback system can be set up between the instrumented collimator and deflection coils just upstream of the radiator, that can operate independent of the crystal alignment system to keep the electron beam aimed at the center of the collimator.

The experimental program in parity violation at Jefferson Lab has already demonstrated a position stabilization circuit that is able to keep the beam position steady to within $20\,\mu m$over a $20\,m$ lever arm. A less sophisticated version of this circuit will meet the position stability requirements for the Hall D photon source.

4.4 Electron beam dump

The electron beam is dumped in the horizontal plane, as shown in figure **??**. The horizontal bend offers several advantages over dumping the beam into the ground. The tagger magnet is easier to support if it sits in the horizontal position. It is also easier to mount and service the focal plane in this position. The dump itself is also more accessible in case it needs to be serviced. An above-ground dump also affords the possibility of running parasitic beam dump experiments that do not interfere with the operation of the experimental hall.

The primary design requirement for the electron beam dump is that it has a sufficiently high capacity to handle beams of the highest intensities foreseen for the GlueX experiment in Hall D. A $60\,kW$ design would provide a a healthy margin for operation of a $12GeV$ beam at $3\,\mu A$ and sufficient capacity to handle $3\,\mu A$at $20GeV$ in the case of a further upgrade.

4.5 Beam containment and shielding

There are three factors that must be taken into account in the design of the shielding for the Hall D beam line. The first is the constraint on the background radiation level that is allowed outside the beam enclosure. The second factor is the level of radiation in the experimental hall which can generate background in the detector during normal running. The third factor is the control of hazards which may occur in the event of a failure of one or more of the beam delivery systems. The first issue has been studied by the Jefferson Laboratory Radiation Controls Group, and will be discussed further in the chapter on Civil Construction. The latter two considerations have been studied by a working group headed by L. Keller (SLAC). A summary of their recommendations [3] follows.

Assuming that the electron beam dump is shielded to the requirements of radiation safety, the next source of background radiation in the experimental hall is the photon collimator. The most penetrating forms of radiation from the collimator are muons and neutrons. A Monte Carlo simulation, assuming a 13 radiation lengths tungsten collimator followed by a sweeping magnet and 5 m of iron shielding, predicted a flux of $1.4 \times 10^3 \mu/\mathrm{s}$ incident on the detector at full operating beam intensity. This is a negligible rate compared with the trigger rate from photon interactions in the target. The flux of neutrons from the collimator is more difficult to calculate, but some fraction of 1 m of concrete shielding will be needed surrounding the collimator enclosure to shield the hall from energetic neutrons.

With regard to hazards associated with the accidental failure of beam line elements or controls, the following measures were recommended in the Keller study [3] and have been incorporated into the HALL D design. The dipole string that bends the electron beam up towards the surface from the below ground and then bends it back horizontal will be connected in series so that failure of a magnet supply or current control electronics cannot result in the beam being steered into the ceiling of the tagger building. The power supply feeding this string of magnets will be protected by a meter relay that shuts off if the current varies from its desired value outside a predefined tolerance. A similar meter relay will also be used on the power supply of the tagger magnet. An electron beam collimator with a burn-through monitor will be located just upstream of the radiator to prevent a mis-steered beam from using radiator support structures as a bremsstrahlung target. Permanent magnets will be located in the upstream region of the photon beam line to bend an errant electron beam into the ground in the case that beam is present while the tagger magnet is off. An emergency beam stop will be installed in the bottom of the photon beam line to catch the errant beam deflected by the permanent magnets. It will be equipped with a current monitor to shut down the primary beam any time electrons are sensed in the photon beam line. Ion chambers located upstream of the photon collimator, and also at the entrance to the photon beam dump behind the experiment, will monitor the total flux in the photon beam and shut off the beam if the flux exceeds a safe value.

List of Figures

List of Tables

Bibliography

[1] J. Benesch. HallD Preliminary Optics Design. Technical Report JLab TN 00-011, Jefferson Lab., 2000.

[2] W. Kaune, G. Miller, W. Oliver, R.W. Williams, and K.K. Young. Inclusive cross sections for pion and proton production by photons using collimated coherent bremsstrahlung. *Phys. Rev.*, D**11**(3):478–494, 1975.

[3] L. Keller. Muon calculation results. Technical Report HallD Note **33**, SLAC, 2000. `http://www.phys.cmu.edu/halld/notes_main.html`.